Composition-Dependent Structural and Electronic Properties of α-(Si1−xCx)3N4

ARTICLE *in* THE JOURNAL OF PHYSICAL CHEMISTRY C · JANUARY 2011

Impact Factor: 4.77 · DOI: 10.1021/jp110109x

8 AUTHORS, INCLUDING:

Ming Xu

Southwest University for Nationalities

103 PUBLICATIONS **661** CITATIONS

SEE PROFILE

Leong Chuan Kwek

National University of Singapore

247 PUBLICATIONS **3,349** CITATIONS

SEE PROFILE

Kostya Ostrikov

The Commonwealth Scientific and Industrial…

521 PUBLICATIONS **8,208** CITATIONS

SEE PROFILE

THE JOURNAL OF PHYSICAL CHEMISTRY C

ARTICLE

pubs.acs.org/JPCC

Composition-Dependent Structural and Electronic Properties of α-$(Si_{1-x}C_x)_3N_4$

M. Xu,[†,#] S. Xu,[‡] M. Y. Duan,[†] M. Delanty,[∥,⊥] N. Jiang,[‡] H. S. Li,[‡] L. C. Kwek,[§] and K. Ostrikov*[,∥]

[†]Key Lab of Information Materials of Sichuan Province & School of Electrical and Information Engineering, South-west University for Nationalities, Chengdu 610041, and International Center for Material Physics, Chinese Academy of Sciences, Shenyang 110016, P. R. China

[‡]Plasma Sources and Applications Center, NIE and Institute of Advanced Studies, Nanyang Technological University, 1 Nanyang Walk, Singapore 637616

[§]NIE and Institute of Advanced Studies, Nanyang Technological University, 1 Nanyang Walk, Singapore 637616

[∥]CSIRO Materials Science and Engineering, P.O. Box 218, Lindfield, New South Wales 2070, Australia

[⊥]Centre for Quantum Information Science and Security, Macquarie University, New South Wales 2109, Australia

ABSTRACT: The highly unusual structural and electronic properties of the α-phase of $(Si_{1-x}C_x)_3N_4$ are determined by density functional theory (DFT) calculations using the Generalized Gradient Approximation (GGA). The electronic properties of α-$(Si_{1-x}C_x)_3N_4$ are found to be very close to those of α-C_3N_4. The bandgap of α-$(Si_{1-x}C_x)_3N_4$ significantly decreases as C atoms are substituted by Si atoms (in most cases, smaller than that of either α-Si_3N_4 or α-C_3N_4) and attains a minimum when the ratio of C to Si is close to 2. On the other hand, the bulk modulus of α-$(Si_{1-x}C_x)_3N_4$ is found to be closer to that of α-Si_3N_4 than of α-C_3N_4. Plasma-assisted synthesis experiments of CN_x and SiCN films are performed to verify the accuracy of the DFT calculations. TEM measurements confirm the calculated lattice constants, and FT-IR/XPS analysis confirms the formation and lengths of C−N and Si−N bonds. The results of DFT calculations are also in a remarkable agreement with the experiments of other authors.

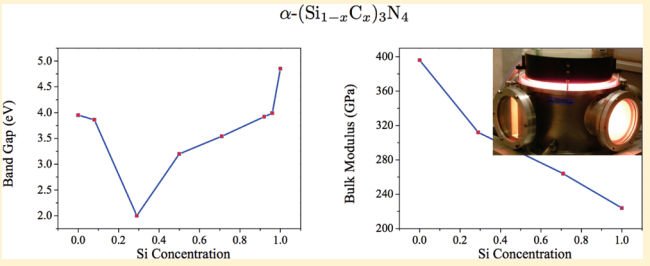

1. INTRODUCTION

Si_3N_4 has been extensively used in microelectronics, optoelectronics, solar cells, machining tools, and the automotive industry because of its excellent physical properties.[1−5] It is well-known that the two stable phases (α and β) of Si_3N_4 possess a hexagonal crystal structure in which all Si atoms are covalently bonded to N atoms in a tetrahedral structure.[6] The third, low-compressibility, and superhard cubic spinel phase (γ-Si_3N_4) was synthesized only in 1999,[7] and its interesting properties were revealed by Ching et al.[8] through first-principles calculations. Meanwhile, carbon nitride (C_3N_4), a material with the same structure as the α- and β-Si_3N_4 phase, is expected to show an extremely high hardness.[9−15] However, it proved very challenging to synthesize high-quality crystalline β-C_3N_4[16−19] with the predicted superhard properties.

In light of these difficulties, attention has turned to silicon carbonitride with a α-Si_3N_4 crystalline structure, which was reported to have a very high hardness.[20] In recent years, experiments have reported on the fabrication, optical and structural characterization, and suggested possible applications of SiCN thin films and nanostructured materials.[21−29] Properties of SiCN materials have also been studied theoretically[21,30] using various approximations of Density Functional Theory (DFT). However, several important questions such as the dependence of the structural constants, electronic structure, and superhard properties on the relative composition of Si and C atoms remain unanswered.

In this work, we elucidate the structural and electronic properties of α-$(Si_{1-x}C_x)_3N_4$ by first-principles DFT calculations, using the presently most accurate Generalized Gradient Approximation (GGA). In particular, we report on the bandgap energy and bulk modulus for a range of carbon concentrations. Our calculations predict unusual behavior of the energy bandgap with carbon concentration. It is also found that the electronic properties of α-$(Si_{1-x}C_x)_3N_4$ are very close to that of α-C_3N_4, whereas the bulk modulus of α-$(Si_{1-x}C_x)_3N_4$ is somewhat closer to that of α-Si_3N_4 than to that of α-C_3N_4. Our experiments on plasma-assisted synthesis and TEM/FT-IR/XPS characterization of CN_x and SiCN films confirm the accuracy of DFT-calculated structural constants and bonding configurations. The DFT-GGA calculations of this work also show a remarkable consistency with the results of other authors.

Received: October 21, 2010
Revised: December 2, 2010
Published: January 5, 2011

Table 1. Comparison of Physical Parameters of α-Si_3N_4, α-$(Si_{1-x}C_x)_3N_4$, and α-C_3N_4

	Si_3N_4				C_3N_4	
	this work	experiments	$(Si_{0.71}C_{0.29})_3N_4$	$(Si_{0.29}C_{0.71})_3N_4$	this work	other calculation
energy (eV)	−11386.86		−11681.54	−12112.56	−12425.16	
a (nm)	0.7675	0.7748[a]; 0.7760[b]	0.7325	0.6963	0.6466	6.4665[e]
b (nm)			0.7411	0.6812		
c (nm)	0.5564	0.5617[a]; 0.5613[b]	0.5325	0.5044	0.4711	4.7097[e]
γ	120°		120.56°	119.99°	120°	
c/a	0.725	0.725[a]; 0.723[b]	0.727	0.724	0.728	0.728[e]
V (nm^3)	0.5675		0.4978	0. 41430	0.3412	
B_0 (GPa)	224	248[c]	264	312	396	425[e]; 351[f]
E_g (eV)	4.85	4.7−4.9[d]	3.54	2	3.95	3.85[e]
ρ (g cm^{-3})	3.30		3.39	3.43	3.57	3.58[e]
Si−N or C−N bond (nm)	0.17202		Si−N: 0.1707 C−N: 0.15067	Si−N: 0.17064 C−N: 0.14723	0.14532	
Si−N or C−N population (average)	Si−N: 0.67		Si−N: 0.67 C−N: 0.75	Si−N: 0.64 C−N: 0.77	C−N: 0.78	
effective charge (e)	Si: 2.15 N: 6.38		Si: 2.13 C: 3.58 N: 6.13	Si: 1.99 C: 3.58 N: 5.66	C: 3.55 N: 5.34	

[a] Ref 32. [b] Ref 33. [c] Ref 34. [d] Ref 35. [e] Ref 10. [f] Ref 36.

2. DFT CALCULATIONS

The DFT calculations in this work use the plane wave pseudopotential (PWP) method and the GGA[30,31] in the CASTEP (Cambridge Serial Total Energy Package) code. By considering a 2 × 1 × 1 $(Si_{1-x}C_x)_3N_4$ supercell, numerical integration of the Brillouin zone is performed using a 2 × 4 × 4 Monkhorst−Pack k-point sampling with the plane wave energy cutoff set at 280 eV. In the optimization process, the energy change, maximum force, maximum stress, and maximum displacement tolerances were set as 1.55 × 10^{-6} eV/atom, 0.035 eV/Å, 0.08 GPa, and 0.002 Å, respectively.

The calculated structural parameters of α-Si_3N_4, α-$(Si_{1-x}C_x)_3N_4$, and α-C_3N_4 crystals found using the GGA method are summarized in Table 1. It is interesting to note that the primitive unit cell for α-Si_3N_4 and α-C_3N_4 structures is hexagonal with $a \approx b$ and $\gamma = 120°$. The optimized structures for α-$(Si_{1-x}C_x)_3N_4$ exhibit a "quasi-hexagonal" configuration with the lattice constant $a < b$ for Si-rich α-$(Si_{1-x}C_x)_3N_4$ and $a > b$ for C-rich α-$(Si_{1-x}C_x)_3N_4$. The angle γ between the unit cell vectors a and b slightly deviates from that of α-Si_3N_4 or α-C_3N_4; i.e., $\gamma > 120°$ for Si-rich α-$(Si_{1-x}C_x)_3N_4$ and $\gamma < 120°$ for C-rich α-$(Si_{1-x}C_x)_3N_4$, contrary to the earlier Local-Density Approximation (LDA) results.[21] The ratio of c to a and the atomic density ρ agree remarkably well with the experimental value and the results of other calculations (see Table 1).

The hardness (bulk modulus B_0, see Figure 1) of α-Si_3N_4, α-$(Si_{1-x}C_x)_3N_4$, and α-C_3N_4 crystals was calculated using the method described by Betranhandy et al.[30] The α-$(Si_{1-x}C_x)_3N_4$ pseudohexagonal structures with $0 < x < 1$ show the magnitudes of hardness to be between those of α-Si_3N_4 and α-C_3N_4. Although the bulk modulus increases and eventually reaches the maximum value intrinsic to the α-C_3N_4 structure as the number of C atoms substituting Si increases, the B_0 values of α-$(Si_{1-x}C_x)_3N_4$ are closer to that of α-Si_3N_4 rather than of α-C_3N_4.[8]

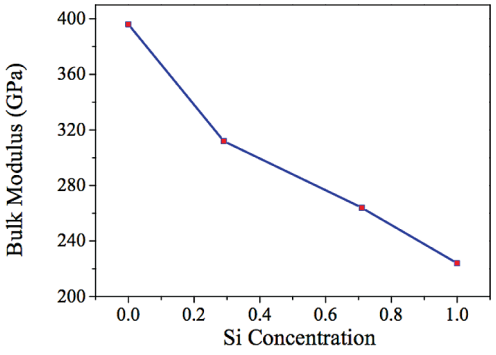

Figure 1. Variation of bulk modulus with silicon concentration in α-$(Si_{1-x}C_x)_3N_4$.

The calculated electronic band structures of α-Si_3N_4, α-$(Si_{1-x}C_x)_3N_4$, and α-C_3N_4 crystals are shown in Figure 2. One can see that both α-Si_3N_4 and α-C_3N_4 are wide-bandgap semiconductors with a direct bandgap (E_g) of 4.85 and 3.95 eV, respectively. The valence band (VB) structures of α-Si_3N_4 and α-$(Si_{1-x}C_x)_3N_4$ crystals are rather similar and distinctly different from the VB of α-C_3N_4. The bandgap of Si-rich α-$(Si_{1-x}C_x)_3N_4$ decreases as the C content in α-$(Si_{1-x}C_x)_3N_4$ increases. The major differences in the band structures are the locations of the states near the conduction band (CB) minimum. The minima of the CB for α-Si_3N_4 and Si-rich α-$(Si_{1-x}C_x)_3N_4$ are located at the G point, while for C-rich α-$(Si_{1-x}C_x)_3N_4$ it is located at the Q point. Alternatively, for the α-C_3N_4 crystal, the CB minimum is located along the $F-Q$ and $Z-G$ directions. Generally the bandgap of α-$(Si_{1-x}C_x)_3N_4$ is smaller than that of either α-Si_3N_4 or α-C_3N_4 and is minimized when $x \sim 0.7$ (see Figure 3). Such variation in E_g is remarkably different from that of γ-$(Si_{1-x}C_x)_3N_4$, for which the bandgap is higher than γ-Si_3N_4 but lower than γ-C_3N_4.[8]

dx.doi.org/10.1021/jp110109x |J. Phys. Chem. C 2011, 115, 2448–2453

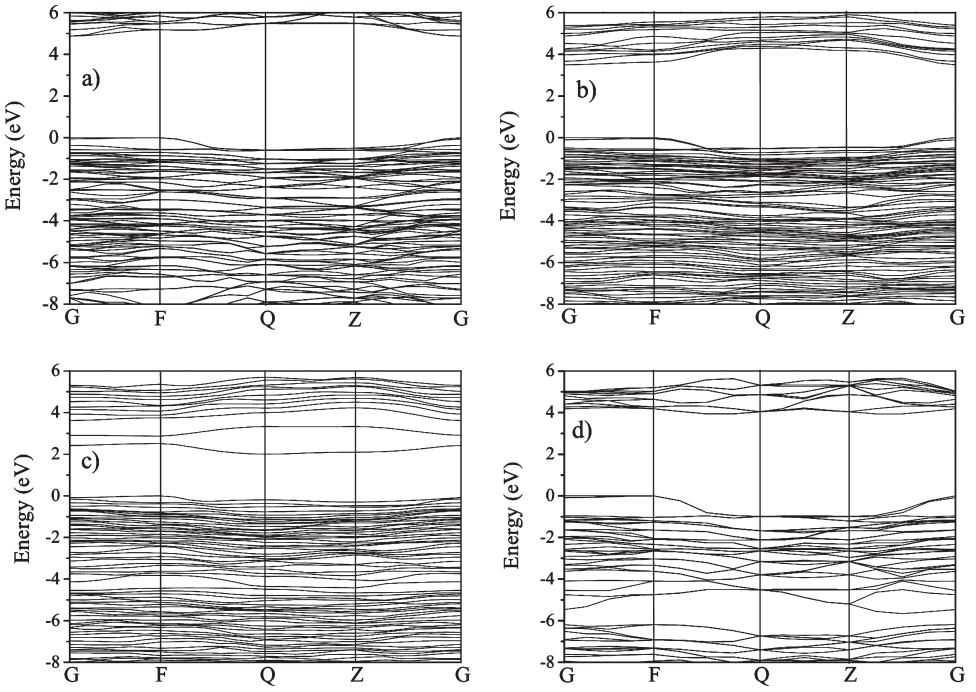

Figure 2. Calculated electronic band structures for (a) α-Si_3N_4, (b) α-$(Si_{0.71}C_{0.29})_3N_4$, (c) α-$(Si_{0.29}C_{0.71})_3N_4$, and (d) α-C_3N_4 crystals.

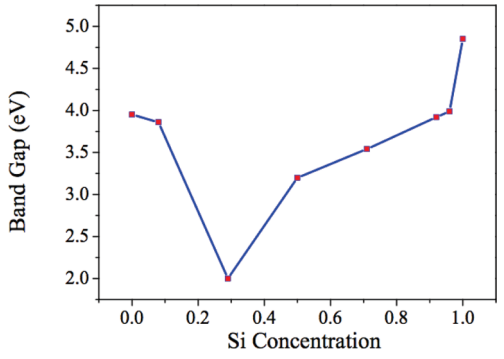

Figure 3. Variation of bandgap with silicon concentration in α-$(Si_{1-x}C_x)_3N_4$.

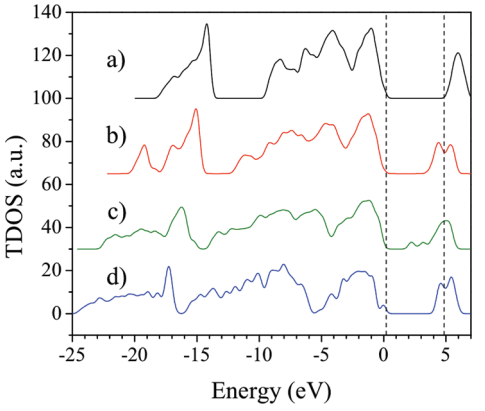

Figure 4. Total DOS of (a) α-Si_3N_4, (b) α-$(Si_{0.71}C_{0.29})_3N_4$, (c) α-$(Si_{0.29}C_{0.71})_3N_4$, and (d) α-C_3N_4 crystals.

Figure 4 presents the calculated total density of states (DOS) for α-Si_3N_4, α-$(Si_{1-x}C_x)_3N_4$, and α-C_3N_4. It is clear that the width of the valence band originated from the s electrons of N monotonously increases with the increase of C concentration. Furthermore, there exists a broad VB between ∼16 and 0 eV, separated by a gap, which decreases with increasing carbon concentration. This larger VB corresponds to the p states of nitrogen, silicon, and carbon. Above 0 eV, one can clearly observe the conduction band populated by the p states of silicon and carbon. The structure of the conduction band of α-$(Si_{1-x}C_x)_3N_4$ shows more similarity to α-C_3N_4 than α-Si_3N_4. We also note that the energy bands become more dispersed when C atoms are introduced. These results suggest that the electronic properties of α-$(Si_{1-x}C_x)_3N_4$ crystals are closer to α-C_3N_4 rather than α-Si_3N_4.

3. EXPERIMENTAL SECTION

To verify the accuracy of the DFT calculations, we have also performed experiments on the synthesis and characterization of CN_x and SiCN films. Carbon-nitride films were deposited on a KCl crystal substrate at ∼70 °C in a plasma-assisted RF magnetron sputtering system.[37] A 10 cm diameter high-purity graphite target was placed on an RF powered electrode in the vacuum chamber with a base pressure of 1.5×10^{-3} Pa. The sputtering process was conducted using 200 W RF power, in a nitrogen plasma at a filling gas pressure of 20 Pa. Typical dissociation rates of nitrogen in the plasma were 15−70%, depending on the electron energy distribution. The SiCN films were deposited by sputtering a Si target in a custom-designed inductively coupled plasma (ICP)-assisted magnetron sputtering system. The N_2 and Ar flow rates were 10 and 4 sccm respectively, while the CH_4 flow rate was varied from 0 to 20 sccm.

The crystalline structure of films was investigated using a SIEMENS D5005 X-ray diffractometer (XRD) with an incident X-ray wavelength of 1.540 Å (Cu Kα line) and also examined by high-resolution transmission electron microscopy (HRTEM)

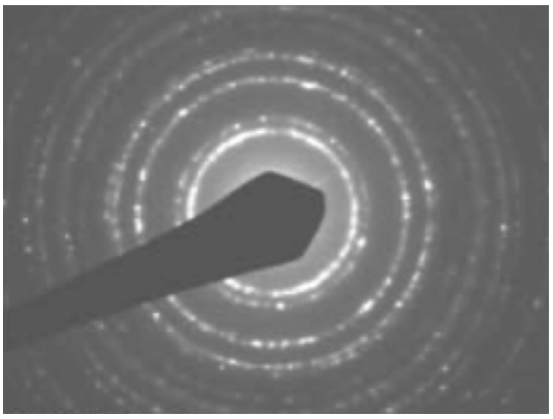

Figure 5. Electron-diffraction pattern of the CN_x film on KBr (100).

Table 2. Comparison of the SAED-Measured Data of α-C_3N_4 with the Predicted Values of Our Calculations

experimental values by SAED		calculated values using a = 0.6466 nm, c = 0.4711 nm in this work	
d (nm)	I	d (nm)	(hkl)
0.3212	s	0.3232	(110)
0.2668	m	0.2665	(111)
0.1878	m	0.1866	(300)
0.1570	m	0.1573	(122)
0.1382	w	0.1369	(203)
0.1249	vw	0.1238	(231)

using a JEOL JEM-2100F TEM. Fourier-Transform Infrared Transmission (FT-IR) analysis was completed with a resolution of 4 cm^{-1} using a NEXUS-670 FTIR spectrometer. The surface chemical composition and bonding states of the films were studied ex situ by a VG ESCALAB 220i-XL spectrometer (XPS) and a Mg Kα (1253.6 eV) X-ray source. Furthermore, the Nanohardness test was carried using Digital Instrument Nanoindenter II (Nano Instrument, Inc.).

The XRD results of the CN_x film show no obvious crystalline peaks in the spectra, while for the SiCN films, there exists a broad diffraction peak between 34° and 37°, which we attribute to the amorphous nature of the SiCN films. The TEM results of the CN_x film on the KBr (100) substrate revealed that this film is of polycrystalline structure (see Figure 5). The corresponding d spacings were calibrated with a single-crystal gold specimen with lattice spacing a = 0.143 nm and c = 0.204 nm and listed in Table 2. The measured lattice spacings in Table 2 are in remarkable agreement with those obtained from the DFT calculations.

Figure 6 displays the IR absorption spectra of CN_x and SiCN films. For the former, two broad absorption bands in the regions of 1200−1700 cm^{-1} and 2900−3500 cm^{-1} and a weak absorption band at ∼2200 cm^{-1} are observed. In general, the absorption of C≡N, C═N, and C−N bonds appears, respectively, at ∼2200, 1500−1600, and 1350−1440 cm^{-1}. Therefore, the deconvoluted peaks at 1348 and 1569 cm^{-1} indicate the existence of single bonds C−N and double bonds C═N in the film. For the SiCN films, the most prominent band (890 cm^{-1}) is

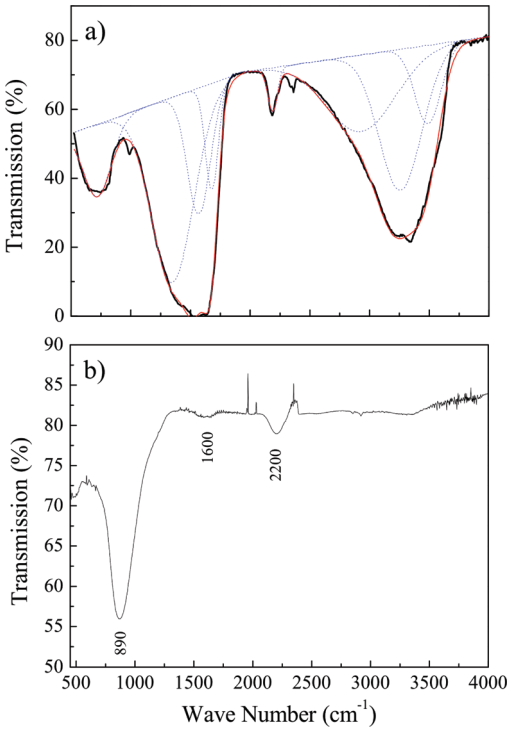

Figure 6. IR absorption spectra of (a) CN_x and (b) SiCN films.

due to the Si−N stretching vibration. Two weak absorption bands in the regions of 2200 and 1600 cm^{-1} are also observed. XPS analysis finds the formation of sp^2 C−N, sp^3 C−N, and Si−N bonds in all the SiCN samples.

The effect of CH_4 flow rate on the nanohardness of the samples was also measured. Increasing the CH_4 flow rate linearly increased the C composition to ∼20% and monotonically reduced the Si and N content. The nanohardness test showed that the increase of the CH_4 flow rate raised the hardness from 12.5 to 15 GPa. The 20% increase of hardness reveals that the incorporation of carbon into SiN_x enhances the hardness, although only marginally.

4. DISCUSSION

Our experiments confirm several conclusions obtained from the DFT calculations. Indeed, from Table 1, it can be seen that the Si−N bond length (0.1706−0.1720 nm) varies in a smaller range than that of the C−N bond (0.1507−0.1453 nm). This indicates that in α-$(Si_{1-x}C_x)_3N_4$ crystals the C−N bond can be stretched or compressed easier than the Si−N bonds. This conclusion is consistent with our experimental results (Figure 6) that suggest various forms of C bonding to N (C−N, C═N, C≡N) are present. We emphasize that the synthesis of an ultrahard C-rich α-$(Si_{1-x}C_x)_3N_4$ crystal with the appropriate amount of C−N bonds is more difficult to implement in practice than that of silicon-rich SiCN. We also note that the calculated crystal lattice constants are in excellent agreement with the experimental values of α-Si_3N_4[32,33] and α-C_3N_4 determined in our experiment (Table 2). Furthermore, the calculated lattice constants for α-C_3N_4 are consistent with the semiempirical approximation of Liu and Cohen[9] and with other experiments.[18,19]

The results of our calculations are also in remarkable agreement with the experimental results of other authors. This can be attributed to the to the high accuracy of the GGA DFT approach.

dx.doi.org/10.1021/jp110109x |J. Phys. Chem. C 2011, 115, 2448–2453

We first compare the calculated and measured bandgap energies of α-$(Si_{1-x}C_x)_3N_4$ crystals. The calculated bandgap of α-Si_3N_4 is ~4.85 eV, which is only 3% smaller than the experimentally measured value of 5.01 eV.[35] This result is much closer to experiment than the previously calculated value of 4.67 eV for α-Si_3N_4.[38] On the other hand, the calculated E_g of the α-C_3N_4 crystal (3.95 eV) is quite close to the 3.85 eV result of Teter.[10]

Experimentally, Chen et al.[20] determined that the bandgap energy of $Si_{35}C_{26}N_{39}$ is 3.81 eV. Our calculations indicate that the bandgap energies of Si-rich α-$(Si_{1-x}C_x)_3N_4$ crystals are between 3.5 and 4.0 eV, in very good agreement with the experimental values. α-Si_3N_4 and Si-rich α-$(Si_{1-x}C_x)_3N_4$ crystals show a direct and wide band gap structure, while C-rich α-$(Si_{1-x}C_x)_3N_4$ crystals possess a smaller but indirect bandgap structure. This suggests that α-Si_3N_4 and Si-rich α-$(Si_{1-x}C_x)_3N_4$ crystals can serve as effective electrical insulators. Moreover, the band structure can be significantly altered by controlled fabrication of nanocrystal (nanoparticle, nanowire, etc.) structures.[39−46]

The calculated hardness of α-Si_3N_4, α-$(Si_{1-x}C_x)_3N_4$, and α-C_3N_4 crystals suggests that this class of materials indeed shows superhard properties.[20,44] Our experimental results show that the amorphous SiCN films possess a bulk modulus comparable to that of α-Si_3N_4. Such variation is in good agreement with that of the calculated hardness of crystalline α-Si_3N_4 and Si-rich α-$(Si_{1-x}C_x)_3N_4$, where the hardness of Si-rich α-$(Si_{1-x}C_x)_3N_4$ is comparable to that of α-Si_3N_4.

5. CONCLUSION

We investigated the physical properties of the α-phase of $(Si_{1-x}C_x)_3N_4$ by DFT calculations based on the GGA approximation. The calculated electronic properties of the α-$(Si_{1-x}C_x)_3N_4$ material with $x < 1$ have been found to be close to those of α-C_3N_4. The introduction of carbon causes the bandgap of α-$(Si_{1-x}C_x)_3N_4$ to significantly decrease and reach a minimum when the ratio of C to Si atoms is approximately 2. Furthermore, our calculations show that the bulk modulus values of α-$(Si_{1-x}C_x)_3N_4$ are closer to α-Si_3N_4 rather than to α-C_3N_4. Our experimental measurements of CN_x and SiCN films verify the calculated lattice constants, and FT-IR/XPS analysis confirms the formation and lengths of various C−N and Si−N bonds. Our results also show a remarkable agreement with the available experimental measurements by other authors. These results suggest that α-$(Si_{1-x}C_x)_3N_4$ materials offer tantalizing prospects for applications as viable electronic and load-bearing materials.

AUTHOR INFORMATION

Corresponding Author

*E-mail: kostya.ostrikov@csiro.au.

Present Addresses

#Institute of Solid State Physics, Sichuan Normal University, Chengdu 610068, P. R. China.

ACKNOWLEDGMENT

This work is supported by the National Research Foundation of Singapore; Sichuan Youth Science & Technology Foundation (Project No. 08ZQ026-025); and the Project-sponsored by SRF for ROCS, SEM, PR China.

REFERENCES

(1) Wang, W.-X.; Li, D.-H.; Liu, Z.-C.; Liu, S.-H. *Appl. Phys. Lett.* **1993**, *62*, 321.
(2) Swain, B. P.; Swain, B. S.; Hwang, N. M. *Appl. Surf. Sci.* **2009**, *255*, 9391.
(3) Herrmann, M.; Schuber, C.; Rendtel, A.; Hübner, H. *J. Am. Ceram. Soc.* **1998**, *81*, 1095.
(4) Levy, J. S.; Gondarenko, A.; Foster, M. A.; Turner-Foster, A. C.; Gaeta, A. L.; Lipson, M. *Nat. Photonics* **2010**, *4*, 37.
(5) Cheng, Q.; Xu, S.; Ostrikov, K. *J. Phys. Chem. C* **2009**, *113*, 14759.
(6) Dufour, G.; Rochet, F.; Roulet, H.; Sirotti, F. *Surf. Sci.* **1994**, *304*, 33.
(7) Zerr, A.; Miehe, G.; Serghiou, G.; Schwarz, M.; Kroke, E.; Riedel, R.; Fuess, H.; Kroll, P.; Boehler, R. *Nature (London)* **1999**, *400*, 340.
(8) Mo, S. D.; Ouyang, L.; Ching, W. Y.; Tanaka, I.; Koyama, Y.; Riedel, R. *Phys. Rev. Lett.* **1999**, *83*, 5046.
(9) Liu, A. Y.; Cohen, M. L. *Science* **1989**, *245*, 841.
(10) Teter, D. M.; Hemley, R. J. *Science* **1996**, *271*, 53.
(11) Swain, B. P.; Swain, B. S.; Hwang, N. M. *Appl. Surf. Sci.* **2009**, *255*, 9264.
(12) Ligatchev, V.; Rusli; Pan, Z. *Appl. Phys. Lett.* **2005**, *87*, 242903.
(13) Niu, C.; Lu, Y. Z.; Lieber, C. M. *Science* **1993**, *261*, 334.
(14) Ball, P. *Nat. Mater.* **2010**, *9*, 701.
(15) Lyth, S. M.; Nabae, Y.; Moriya, S.; Kuroki, S.; Kakimoto, M. -A.; Ozaki, J. -I.; Miyata, S. *J. Phys. Chem. C* **2009**, *113*, 20148.
(16) Yin, L. -W.; Bando, Y.; Li, M. -S.; Liu, Y. -X.; Qi, Y. -X. *Adv. Mater.* **2003**, *15*, 1840.
(17) Xu, S.; Kumar, S.; Li, Y.-A.; Jiang, N.; Lee, S. *J. Phys.: Condens. Matter* **2000**, *12*, L121.
(18) Xu, S.; Li, H.-S.; Li, Y.-A.; Lee, S.; Huan, C. H. A. *Chem. Phys. Lett.* **1998**, *287*, 731.
(19) Li, Y.-A.; Xu, S.; Li, H.-S.; Luo, W.-Y. *J. Mater. Sci. Lett.* **1998**, *17*, 31.
(20) Chen, L. C.; Chen, C. K.; Wei, S. L.; Bhusari, D. M.; Chen, K. H.; Chen, Y. F.; Jong, Y. C.; Huang, Y. S. *Appl. Phys. Lett.* **1998**, *72*, 2463.
(21) Chen, C. -W.; Huang, C.-C.; Lin, Y.-Y.; Su, W.-F.; Chen, L.-C.; Chen, K.-H. *Appl. Phys. Lett.* **2006**, *88*, 073515.
(22) Du, X.-W.; Fu, Y.; Sun, J.; Yao, P. *J. Appl. Phys.* **2006**, *99*, 093503.
(23) Su, D.; Li, Y. -L.; Feng, Y.; Jin, J. *J. Am. Ceram. Soc.* **2009**, *92*, 2962.
(24) Swatowska, B.; Stapinski, T. *Phys. Status Solidi (C)* **2010**, *7*, 758.
(25) Awad, Y.; El Khakani, M. A.; Scarlete, M.; Aktik, C.; Smirani, R.; Camiŕ, N.; Lessard, M.; Mouine, J. *J. Appl. Phys.* **2010**, *107*, 033517.
(26) Swain, B. P.; Hwang, N. M. *Appl. Surf. Sci.* **2008**, *254*, 5319.
(27) Jedrzejowski, P.; Cizek, J.; Amassian, A.; Klemberg-Sapieha, J. E.; Vlcek, J.; Martinu, L. *Thin Solid Films* **2004**, *447−448*, 201.
(28) Guthy, C.; Das, R. M.; Drobot, B.; Evoy, S. *J. Appl. Phys.* **2010**, *108*, 014306.
(29) Baraton, M. -I.; Chang, W.; Kear, B. H. *J. Phys. Chem.* **1996**, *100* (41), 16647–16652.
(30) Betranhandy, E.; Capou, L.; Matar, S. F.; El-Kfoury, C. *Solid State Sci.* **2004**, *6*, 315.
(31) Duan, M.-Y.; He, L.; Xu, M.; Xu, M.-Y.; Xu, S.; Ostrikov, K. *Phys. Rev. B* **2010**, *81*, 033102.
(32) Hardie, D.; Jack, J. H. *Nature* **1957**, *180*, 332.
(33) Priest, H. F.; Burns, F. C.; Priest, G. L.; Shaar, E. C. *J. Am. Ceram. Soc.* **1973**, *56*, 395.
(34) Yeheskel, O.; Gefen, Y. *Mater. Sci. Eng.* **1985**, *71*, 95.
(35) Carson, R. D.; Schnatterly, S. E. *Phys. Rev. B* **1986**, *33*, 2432.
(36) Guo, Y.; Goddard, W. A. *Chem. Phys. Lett.* **1995**, *237*, 72.
(37) Xu, S.; Ostrikov, K.; Long, J. D.; Huang, S. Y. *Vacuum* **2006**, *80*, 620.
(38) Xu, Y. -N.; Ching, W. Y. *Phys. Rev. B* **1995**, *51*, 17379.

(39) Cvelbar, U.; Chen, Z.; Sunkara, M. K.; Mozetic, M. *Small* **2008**, *4*, 1610.
(40) Hwang, N. M.; Swain, B. S.; Swain, B. P. *J. Phys. Chem. C* **2010**, *114*, 15274.
(41) Xu, M.; Xu, S.; Huang, S. Y.; Chai, J. W.; Ng, V. M.; Long, J. D.; Yang, P. *Phys. E* **2006**, *35*, 81.
(42) Ostrikov, K. *Rev. Mod. Phys.* **2005**, *77*, 489.
(43) Bian, S. -W.; Ma, Z.; Song, W. -G. *J. Phys. Chem. C* **2009**, *113*, 8668.
(44) Mélinon, P.; Masenelli, B.; Tournus, F.; Perez, A. *Nat. Mater.* **2007**, *6*, 479.
(45) Wnuk, J. D.; Gorham, J. M.; Fairbrother, D. H. *J. Phys. Chem. C* **2009**, *113*, 12345.
(46) Ishikawa, T.; Kohtoku, Y.; Kumagawa, K.; Yamamura, T.; Nagasawa, T. *Nature* **1998**, *391*, 773.